frontiers | Frontiers in Materials

TYPE Original Research
PUBLISHED 20 February 2024
DOI 10.3389/fmats.2024.1360869

OPEN ACCESS

EDITED BY
Wenwen Dou,
Shandong University (Qingdao), China

REVIEWED BY
Zhong Li,
Northeastern University, China
Dake Xu,
Northeastern University, China

*CORRESPONDENCE
R. K. Singh Raman,
raman.singh@monash.edu

RECEIVED 24 December 2023
ACCEPTED 07 February 2024
PUBLISHED 20 February 2024

CITATION
Welikala S, Al-Saadi S, Gates WP, Panter C and Singh Raman RK (2024), Sulphate reducing bacteria (SRB) biofilm development and its role in microbial corrosion of carbon steel. *Front. Mater.* 11:1360869.
doi: 10.3389/fmats.2024.1360869

Sulphate reducing bacteria (SRB) biofilm development and its role in microbial corrosion of carbon steel

Sachie Welikala[1], Saad Al-Saadi[1,2], Will P. Gates[3], Christopher Panter[4] and R. K. Singh Raman[1,2]*

[1]Department of Chemical and Biological Engineering, Monash University, Clayton, VIC, Australia, [2]Department of Mechanical and Aerospace Engineering, Monash University, Clayton, VIC, Australia, [3]Institute for Frontier Materials, Deakin University, Burwood, VIC, Australia, [4]CP Microbiology and Analytical Laboratories, Mulgrave, VIC, Australia

The development of biofilm by pure SRB culture on carbon steel, and its role on corrosion were investigated using microscopic, spectroscopic, electrochemical and surface characterization techniques. Tubercle biofilm and irregularly shaped pits were observed on steel surfaces in high-nutrient biotic solution. Owing to development of a protective FeS film in 72 h immersion, corrosion resistance improved. In nutrient-deficient medium, a greater bacterial density attached to the metal surface as the consequence of starved bacteria seeking energy sources from metal. However, electrochemical non-homogeneity developed at the locations of their attachment, that gradually grew over the entire surface.

KEYWORDS

sulphate reducing bacteria (SRB), focused ion beam-scanning electron microscopy (FIB-SEM), environmental scanning electron microscopy (ESEM), microbial corrosion, biofilm

1 Introduction

Microbiologically influenced corrosion (MIC) is a considerable concern in various industries; water systems, marine transport and structures, oil and gas production, power generation, storage are just a few (Little and Lee, 2007; Little et al., 2020). MIC is a serious problem particularly in pipelines, pumps and de-aeration towers of the oil and gas industry. The major source of bacterial contamination in the oil and gas industry is the return water which is injected into oil reservoirs in large amounts (e.g., 600,000 barrels/day) to maintain pressure in the well during secondary recovery (Allsopp et al.). The well-known example is the MIC causing pipeline rupture that led to a fire in New Mexico in 2000 (Xu and Gu, 2014). Failures due to MIC was also the prime suspect for the escape of more than 100,000 tons of methane from a well casing in a storage field in Aliso Canyon, CA, United States, and leakage of 750,000 L of oil from the pipeline in Prudhoe Bay, Alaska (Little et al., 2020). Revenue loss due to MIC is generally estimated to be between 1% and 5% of Gross National Product in developed countries (Revie, 2008; Little and Lee, 2009), and the cost of MIC has been estimated to be 20% of the total cost of corrosion (Little and Lee, 2007; Javaherdashti, 2017). The cost of corrosion can be divided into direct and indirect costs (Revie, 2008; Johnston and Voordouw, 2012).

Carbon steel is widely used in various industries. It is also the most commonly used metallic material in the oil and gas industry (Heidersbach, 2018) due to low cost and

TABLE 1 Chemical composition of the commonly used Postgate C, modified Postgate C and inorganic Postgate C solutions.

Chemicals	Postgate C	Modified Postgate C	Inorganic Postgate C
Na_2SO_4[a]	4.5	4.5	4.5
$CaCl_2 .2H_2O$[a]	0.06	0.06	0.06
Lactic acid[b]	4.8	4.8	
Sodium citrate[a]	0.3	0.3	
NH_4Cl[a]	1.0	1.0	1.0
K_2HPO_4[a]	0.5	0.5	0.5
$MgSO_4 .7H_2O$[a]	2.0	2.0	2.0
Yeast extract[a]	1.0		

a: concentration in g/L. b: concentration in mL/L.

TABLE 2 Chemical composition of the carbon steel coupons used in the electrochemical studies (% by weight, balance Fe).

Elements	C	Si	Mn	P	S	Al	Cu	Cr	Ni	Mo	Fe
(% by weight)	0.14	0.20	1.22	0.022	0.025	0.005	0.008	0.030	0.01	0.03	Balance

adequate mechanical properties (Revie, 2008). However, carbon steel suffers from MIC in several industries. Formation of a bacterial biofilm plays a crucial role in the corrosion characteristics of carbon steel (Papavinasam, 2013; Enning and Garrelfs, 2014). The bacteria type that are most commonly reported to accelerate corrosion processes are the sulphate reducing bacteria (SRB), such as *Desulfovibrio desulfuricans* (Little and Lee, 2014). SRB can alter the characteristics of the metal/solution interface due to their metabolic processes, such as by excreting extra cellular polymeric substances (EPS), setting up gradients of pH or oxygen or through the formation of iron sulphide films (Enning and Garrelfs, 2014). The formation of hydrogen sulphide due to SRB, which precipitates as iron sulphides, plays an important role in indirectly influencing the corrosion process of carbon steel in SRB containing environments. The limited number of studies carried out on carbon steel exposed to SRB under limited organic carbon nutrient conditions observed increased localized corrosion. However, most laboratory media used in MIC investigations contained high organic carbon nutrient contents (Little et al., 2007), which may not represent conditions in industrial waters. It is crucial to note that SRB is an anaerobic type of bacteria that may undergo aggressive metabolic activities under starvation conditions. Such a condition is not entirely simulated/represented in the high organic carbon nutrient containing mediums that have generally been employed in earlier investigations.

The objective of this work was to investigate the effect of biofilms developed by SRB on corrosion characteristics of carbon steel. Biofilms formed by a representative SRB (*D. desulfuricans*) were investigated using microscopic observation, chemical characterisation and electrochemical techniques. As the environmental conditions available to the bacteria have inimical effect on the biofilm development and corrosion processes, the organic nutrients supply to the bacteria was adjusted accordingly. Therefore, the biofilms were developed under i) high organic nutritional environment such as the commonly used Postgate C medium, moderate decrease of organic nutrients by the removal of nutrient, yeast extract (modified Postgate C medium) and ii) starvation conditions, where all organic nutrients were removed from the environment (inorganic medium). The biofilms developed on carbon steel for 72 h and 168 h in different environmental conditions (commonly used Postgate C medium, modified Postgate C medium and inorganic medium) were investigated in pure culture of SRB. Open circuit potential (OCP), linear polarization (LP) and potentiodynamic polarization (PDP) tests were used for characterization of corrosion. Environmental scanning electron microscopy (ESEM) was used to study the morphologies of the biofilm on carbon steel. FIB-SEM is a potent technique to characterize the cross-section and microstructure of biofilms (Steve and Robert, 2001; Cui et al., 2020; Li et al., 2020). Applying FIB-SEM, Li et al. (Li et al., 2020) studied the bacterial distribution in SRB biofilm, and observed the morphology of bacterium cells and corrosion product layers that affected MIC/pitting of carbon steel. In the present study, FIB-SEM was employed for comprehensive examination of cross-sections of SRB biofilm and MIC to characterize the sub-surface features of SRB biofilms under different nutrient conditions (i.e., nutritionally rich, as compared to nutritionally deficient). Attenuated Fourier transformation infrared spectroscopy (ATR-FTIR) was also used, together with microscopic and electrochemical techniques, to examine the bacterial extracellular polymeric substances (EPS).

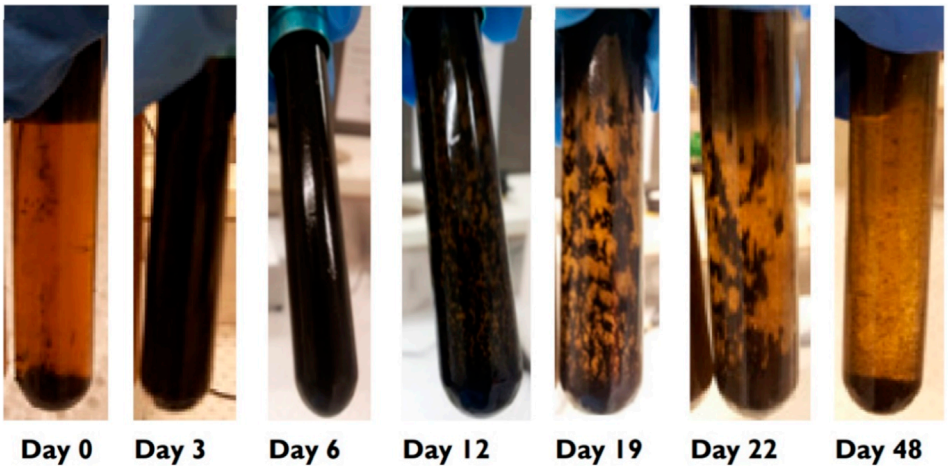

FIGURE 1
Desulfovibrio desulfuricans growth in B7 medium showing initial iron sulphide formation on the glass wall, and eventual breakdown of this coating due to the crystal size enlargement and nutrient limitations.

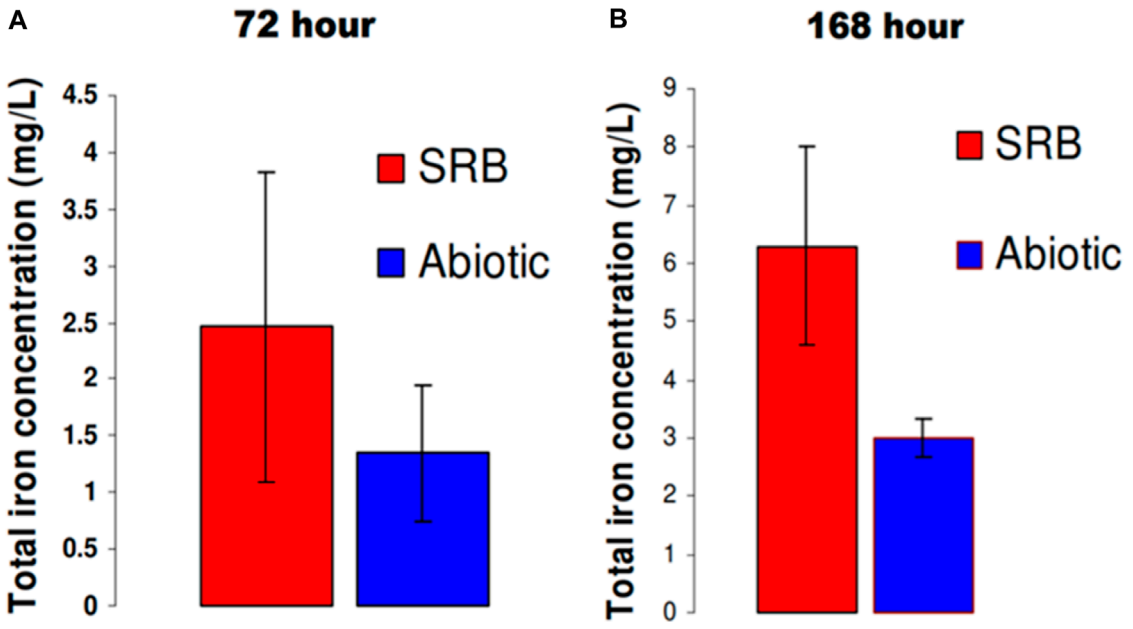

FIGURE 2
Quantification of total iron (Fe^{2+} and Fe^{3+}) in solution after: **(A)** 72 h and **(B)** 168 h in modified Postgate C medium.

2 Experimental procedure

2.1 Bacterial culture

SRB is cultivated reliably in B7 medium at a mesophillic temperature of 30°C. As compared to other media, Postgate B is generally believed to be more suitable for studies on SRB (Jain, 1995). The chemical composition of the B7 medium was (/L): 0.8 g K_2HPO_4, 0.2 g KH_2PO_4, 0.2 g $MgSO_4$, 5 g yeast extract, 5 g peptone, 10 g ferric ammonium citrate, 10 mL $CaSO_4$ (saturated solution). The pH of the medium was adjusted to 7.5–7.8. The pure bacterial culture of SRB was grown in test tubes under anaerobic conditions and the growth of the SRB is confirmed by the formation of black iron sulphides in suspension and in precipitate. To avoid contamination of the enrichment cultures, all lab glassware, pipettes, and solution were sterilised at 121°C for 15 min. The purity of the cultures was monitored by regular observation of the bacterial cells under the phase contrast microscope. The cultures were periodically renewed to keep them active and healthy. A 1 mL sample of a 3-day old inoculum was taken from the culture for biofilm development and electrochemical experiments.

10.3389/fmats.2024.1360869

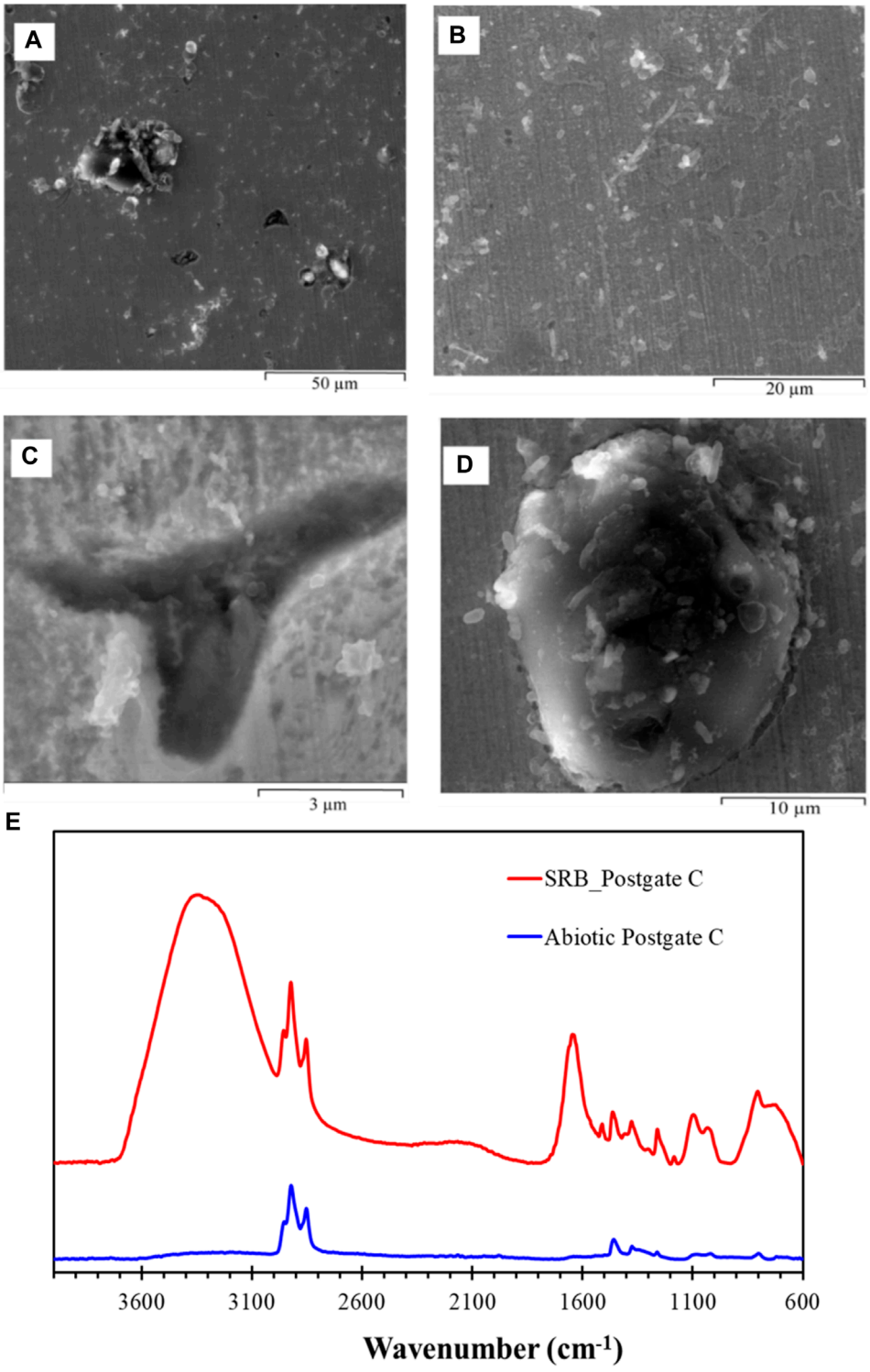

FIGURE 3
ESEM images of hydrated biofilm formed on carbon steel by a pure SRB culture following 72 h exposure in Postgate C medium. **(A)** An overview image of the biofilm showing the heterogeneous distribution of pits and precipitates, **(B)** area showing a thin adherent film, **(C)** irregular shaped pits were observed scattered throughout the specimen, and **(D)** tubercle structure in the biofilm. **(E)** IR spectrum of SRB biofilm formed on carbon steel exposed to a pure SRB culture in Postgate C medium for a period of 72 h and abiotic Postgate C medium.

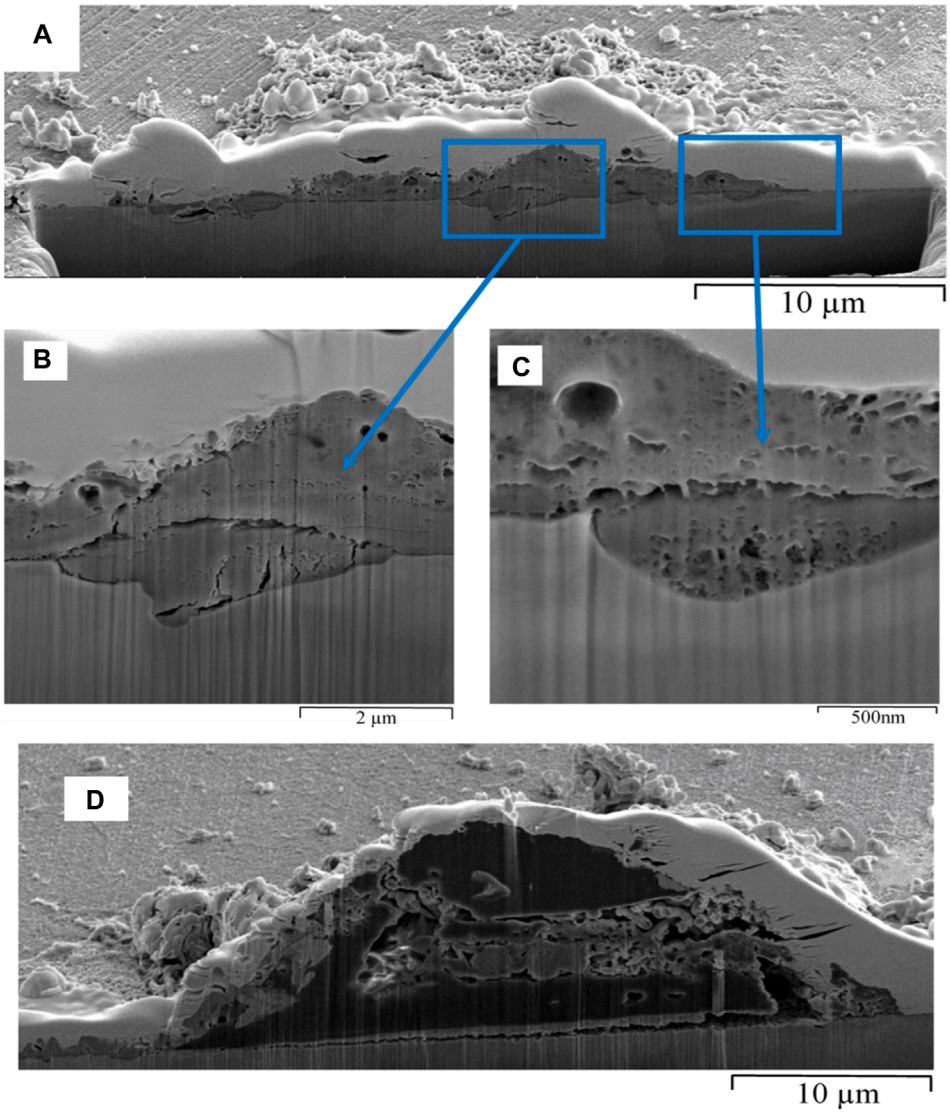

FIGURE 4
FIB-SEM cross-section of biofilm formed on carbon steel by pure culture of SRB in Postgate C medium following a 72 h exposure: **(A)** an overview image of the cross-section and **(B)** and **(C)** a closer look at the porosity in the corroded areas, and **(D)** cross-section of a tubercle structure found on the surface of a 72 h SRB biofilm in Postgate C medium.

2.2 Test solutions

Three recipes of Postgate C medium were prepared for biofilm development and corrosion characterization (i.e., commonly used Postgate C, modified Postgate C and inorganic Postgate C solutions). The composition of all Postgate C solutions used in the present study is summarized in Table 1. Postgate C medium has been generally used to evaluate the effect of SRB on steels using different electrochemical measurements (Al-Saadi, 2013). Another advantage of Postgate C medium is that the resulting solutions were clear, which is better suited for mass culturing of SRB as well as for continuous culture (since the turbidity of other media often makes observations difficult) (Al-Saadi, 2013; Videla, 2018). The modified Postgate C medium was prepared by removing the yeast extract from the medium for the purpose of moderately decreasing the amount of organic nutrients available to the bacteria. The inorganic medium was prepared by completely removing all organic ingredients in the media in order to study the behaviour of the bacteria under starvation conditions. The pH of the culture media was adjusted to 7.5–7.8 using sterilised NaOH solution, and all solutions were autoclaved to avoid contamination. No iron component was included in the test medium for electrochemical testing or for biofilm study. The iron in solution as measured by the 1, 10 phenanthroline method originated from the dissolution of the carbon steel specimen.

2.3 Carbon steel samples

The working electrodes were made of grade 250 carbon steel (procured from Bluescope steel) with the composition as shown in

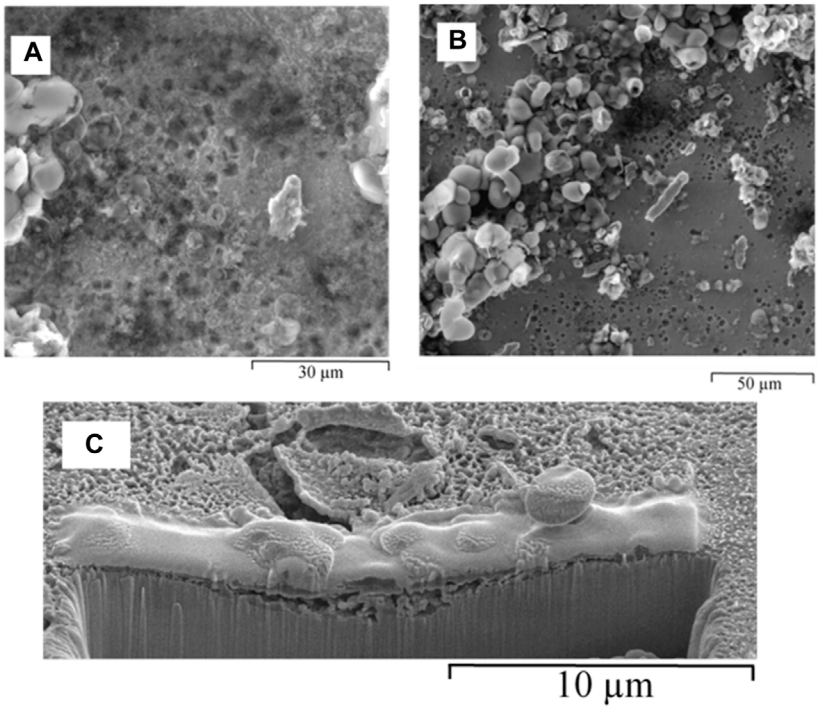

FIGURE 5
ESEM images of hydrated biofilm formed on carbon steel by a pure SRB culture following 168 h exposure in Postgate C medium: **(A)** small round pits, and **(B)** heterogeneous distribution of corrosion products, showing bulky deposits alongside tightly adherent film and shallow pitting. **(C)** FIB-SEM, cross-section of biofilm formed due to pure culture of SRB in Postgate C medium following a 168 h exposure.

Table 2. For electrochemical tests, the preparation of the working electrode is described in detail in (Al-Saadi, 2013; Al-Saadi et al., 2017; Al-Saadi and Raman, 2019). A copper wire was soldered to the underside of a square specimen of carbon steel (coupon). The wire was encased in a glass tube to prevent any contact of the wire with the electrolyte. Each specimen was then mounted in epoxy resin so that only the upper face of the steel coupon was exposed to the test solution. The surface was wet ground with emery paper sequentially from 120, 180, 320, 600 and 1,200 grit and then polished with diamond paste to 3 µm. The edges of the resin and the metal were painted with an enamel coating to avoid crevice corrosion (Cheng et al., 1998; Al-Saadi, 2013; Al-Saadi et al., 2017; Al-Saadi and Raman, 2019). For microscopic investigations, a fishing line was used to hang the sample in the test solution, and no copper wire was used. The samples were ultrasonically cleaned for 15 min in ethanol prior to being used as test electrodes in electrochemical experiments or in immersion tests for biofilm characterization.

2.4 Iron quantification

Ferrous and ferric ion concentration is directly relevant to the corrosion characteristics of carbon steel. Accordingly, the total iron (Fe^{2+} and Fe^{3+}) concentrations in this study was determined using a colorimetric technique using 1, 10-phenanthroline following the procedure outlined in reference (American Public Health et al., 2005).

2.5 Microscopy and spectroscopy of biofilm cross-sections

2.5.1 Development of biofilms on carbon steel for microscopic imaging and FIB-SEM analysis

The carbon steel coupons, mounted in epoxy resin and attached to a polypropylene fishing line (as described in Section 2.3), were immersed in 250 mL of sterilized test solutions (either Postgate C medium, modified Postgate C medium or Inorganic medium) in a 250 mL Duran bottle. Using aseptic techniques, 1 mL of bacterial culture was taken from a 3-day old stock culture of SRB and inoculated into the Duran bottle as pure culture. The solution was not de-aerated. A layer of paraffin was then placed on the top of the solution, with a view to maintaining anaerobic conditions once these were established over the course of the experiment. Growth of the introduced SRB strain confirmed that anaerobiosis developed within the 72 h period. An abiotic control was also set up under the same conditions. The carbon steel specimen was exposed to the bacterial culture (or abiotic conditions) for a period of 72 h or 168 h at 30°C. At least two samples were observed for each condition in order to check for the reproducibility.

2.5.2 Biofilm fixation and environmental scanning electron microscopy (ESEM) imaging

The morphology of the biofilm on the carbon steel specimen was observed using the 3D Quanta FEI in ESEM mode. Biofilms were fixed using 2% glutaraldehyde solution for 1 h and then subjected to 2 washes in deionised water, each wash for 5 min. The use of

relatively high pressures (~650 Pa, or 1 mbar) and water vapor in the specimen chamber in the ESEM allowed the samples to be viewed in a hydrated state, and without the need for metallic coating that is often required in SEM sample preparation which could introduce artifacts to the biofilms. At least two samples were observed under ESEM for each condition.

2.5.3 Focused ion beam–scanning electron microscopy (FIB-SEM)

FIB-SEM technique was used to investigate sub-surface features of the biofilm. FIB milling was carried out using the FEI Quanta 3D FEG instrument. As this instrument also has SEM and EDS capabilities, the subsurface structure could be viewed, and elemental composition analysed following the milling. As the sample was placed in a high vacuum chamber (~10^{-6} Pa), in addition to the sample preparation steps detailed in Section 2.5.2 for ESEM, the sample was also dehydrated, and sputter coated with 3 nm of platinum coating in order to avoid charging. The surface of the specimen was first viewed under SEM to locate a site of interest in the biofilm for subsequent cross-sectional analysis. The site chosen for FIB-milling was typical and representative for the condition under study. A platinum strip, 1 µm in width and 1 µm in thickness, was applied across the length of the area of interest in order to protect the biofilm from ion beam degradation during the milling process (Blankemeier, 2011). The sample was then tilted to 52° so that the milling could be performed using a gallium (Ga^+) beam with the current in the range of 5 nA. Beam currents were lowered (to the pA range) for subsequent cleaning of the cross-sections for removing material re-deposited on the area during the initial rough milling.

2.5.4 Attenuated total reflectance–fourier transform infrared (ATRFTIR) spectroscopy

The specimens exposed to biotic and abiotic conditions were removed after 72 h and any loosely attached bacterial cells were rinsed off with phosphate buffer solution. The specimens were left in a desiccator for at least 24 h to dehydrate. FTIR spectra were obtained using a Perkin Elmer Spectrum 100 series spectrometer. The spectral acquisition (128 co-added scans at 8 cm^{-1} of spectral resolution in the 4,000 cm^{-1} to 600 cm^{-1} range) were obtained by pressing the exposed steel surface to the ATR crystal and spectral processing was done using Perkin Elmer Spectrum Express software. Background scans, consisting of the clean pressure applicator against the ATR crystal, were acquired prior to scanning of each specimen.

2.6 Electrochemical measurements

Linear polarization (LP) and potentiodynamic polarization (PDP) were carried out using a Princeton Applied Research Potentiostat (model: 2,273) and a three-electrode electrochemical cell. The test cell was a 250 mL Duran bottle filled with 250 mL of the test solution (Postgate C medium, modified Postgate C medium or the Inorganic medium). The design of the electrochemical cell is described elsewhere (Al-Saadi, 2013; Al-Saadi et al., 2017; Al-Saadi and Raman, 2019; Al-Saadi et al., 2021a). The steel coupons were used as the working electrodes, saturated calomel electrode (SCE) was used as the reference electrode and a platinum mesh was used as the counter electrode. As for other experiments, following the immersion of the three electrodes in the test solution, a paraffin layer was placed on top to allow the development of anaerobic conditions. The Duran bottle was then tightly sealed. Paraffin is not completely impermeable to oxygen. However, strictly anaerobic conditions were not required for SRB. The formation of black iron sulphide precipitates in the SRB inoculated medium was taken as confirmation that sufficient anaerobic conditions were set up in the test solution. The paraffin layer was carefully drained when samples were taken out of the test cell for examination as to avoid contaminating the sample with oil. For the biotic electrochemical experiments, 1 mL of inoculum from the maintenance culture was introduced into the test solution. Abiotic control experiments were also conducted alongside the biotic experiments. All the measurements were repeated at least thrice to examine reproducibility. Open circuit potential (OCP) was monitored for at least 1 h to confirm its stability with time. For LP test, the working electrode was polarized ±10 mV from E_{corr} at a scan rate of 0.166 mV/s. Potentiodynamic polarization was carried out at a scan rate of 1 mV/s, starting at a potential of 400 mV more negative to the OCP.

3 Results and discussion

3.1 Iron and sulphide measurements in solution

The culture media provided electron acceptor, sulphate, for the bacteria in test solution and in the enrichment B7 media. The SRB instantaneously reduced this sulphate to sulphide using organic carbon (or molecular hydrogen) as the electron donor. The formation of iron sulphides, which was taken as a sign of positive SRB growth, could also be observed visually due to darkening of the solution. Eq. (1) describes iron sulphide formation in a biotic solution due to the oxidation of iron and generation of hydrogen sulphide (Castaneda and Benetton, 2008).

$$Fe^{2+} + H_2S = FeS + 2H^+ \quad (1)$$

These iron sulphides also precipitated on the surface of the carbon steel coupon and resulted in blackening of the steel surface. It was observed that the Postgate C medium, which contains a high organic nutrient content, was the most favourable of the three-growth media used in corrosion tests for the SRB. Solution blackening and strong H_2S odour occurred within 48 h. Deep blackening of the solution also occurred in the modified Postgate C medium during 96–120 h exposure period. The inorganic medium was, however, inufficient for rapid growth and considerably lower amounts iron sulphide formation were visually observed.

Figure 1 follows the iron sulphide formation in test tubes of the enrichment culture (B7 medium). The heaviest blackening occurred between day 3–6 when the bacteria were the most active. Small iron sulphide crystals precipitate on the walls of the test tube during day 3–6 due to the large surface area-to-volume ratio. These iron sulphide crystals eventually began to detach from the test tube wall from day 12 onwards due to crystal growth which decreased

surface area to volume ratio and thereby diminished the force at which the iron sulphides are held onto the glass wall. Previous studies have shown that concentrations above 500 mg SO_3^{2-}/L inhibit growth of SRB (van Houten). Following 48 days incubation, the iron sulphide settled at the bottom of the test tube and the solution appeared clearer. When observed under the phase contrast microscope, planktonic cells for the following 48 days appear in cocci shape and non-motile. However, these cells were still viable. Once provided with sufficient nutrients, they could be revived.

Quantification of the amount of iron corroded from the steel coupon was carried out using the 1, 10 phenanthroline method following exposure to SRB. Figure 2 shows that ≈2x higher concentration of dissolved iron in solution was present when carbon steel was exposed to SRB than to the abiotic conditions. Iron oxides formed on the carbon steel coupon may have resulted in lower dissolved iron for the sample exposed to abiotic conditions as compared to the SRB.

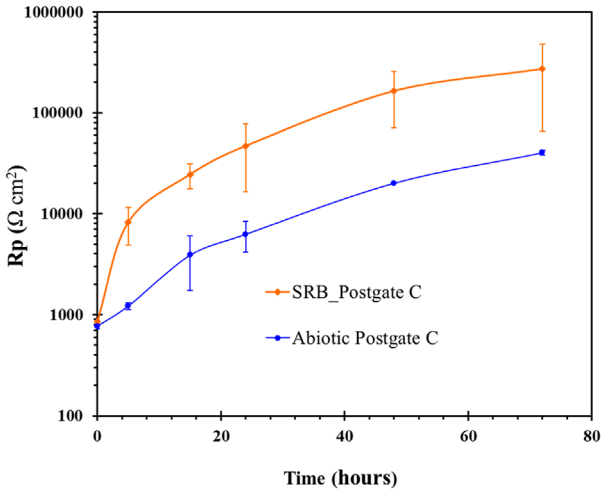

FIGURE 6
Linear polarisation resistance of carbon steel exposed with and without a pure SRB culture in common Postgate C medium.

3.2 Biofilm and electrochemical characterization of carbon steel exposed to commonly used Postgate C medium with SRB

3.2.1 Biofilm characterization in Postgate C solution

Postgate C medium allowed reliable and rapid growth of *D. desulfuricans* due to its high organic nutrient content. Pits were found sparsely throughout the carbon steel following a 72 h exposure to the SRB (Figures 3A,B). Although earlier studies have reported that pit morphology in the presence of SRB occurred as disc shaped concentration cells (Videla, 1987), the pits observed in this study were irregular-shaped and did not follow a distinctive trend (Figure 3C). Another distinctive feature in the SRB biofilm was the presence of tubercle structures (Figure 3D). When cultured in the nutrient-rich Postgate C medium, bacterial cells were not observed to be attached to the carbon steel surface. They were either well hidden within corrosion product layers or did not attach to the carbon steel due to favourable growth conditions in the bulk solution. In the latter case the iron sulphide deposited on the film would have formed due to the H_2S production by planktonic (free-floating) SRB cells. Xu et al. (Xu et al., 2023) reported that planktonic cell numbers had no impact on MIC pitting attack as they did not utilise electrons from the iron dissolution reaction for the reduction of sulphate and oxidation of organic carbon nutrients. EDS elemental analysis detects carbon, oxygen, sulphur, phosphorous, silicon, manganese and iron on 72 h SRB biofilm on carbon steel (Figure S1 in supplementary document).

Figure 3E shows the FTIR spectra of SRB biofilm on carbon steel exposed to biotic solution and the film formed during exposure to abiotic medium for a period of 72 h. A much stronger IR signal could be obtained for the SRB biofilm as compared to the abiotic Postgate C medium. The presence of organic compounds in the film can be readily identified by the absorption bands between 2,956–2,852 cm^{-1}, accounting for the CH_3 and CH_2 functional groups from the aliphatic chains in lipids (Coates, 2000; Ramesh et al., 2006). Complementary bands supporting the presence of C-H peaks were found in the region between 1,462 and 1,378 cm^{-1}, where bending vibrations of the -CH_3 and -CH_2 groups occur (Naumann and John WileySons, 2006; Ojeda et al., 2009). A broad absorption band near 3,320 cm^{-1} in the SRB biofilm in Postgate C arose from the stretching vibration of hydroxyl groups of structurally bound water in iron oxyhydroxides, or possibly proteins (Ramesh et al., 2006). This broad peak was most prominent in the pure SRB culture biofilm than any other biofilm investigated in this study. Structurally bound water can occur during rapid precipitation of iron oxyhydroxides where chemisorbed/dissociated water molecules at the mineral surface may be trapped within the crystalline mineral. This leaves excess hydroxyl surrounding the lattice site where Fe^{2+} ion would otherwise be found. When temperatures are sufficiently low to impede the diffusion of H or OH out of the material, this excess hydroxyl level can increase and be stabilised through structural phase transformation (Pinney and Morgan, 2013).

The N-H stretch bands of amides occur in the region 3,300–3,000 cm^{-1} and overlap with the broad peak of OH stretching. Therefore, the region between 1800 and 1,500 cm^{-1} were used to identify proteins as it is dominated by conformation sensitive amide I and amide II bands (Naumann and John WileySons, 2006). The exact frequency of amide band vibrations is determined by the secondary structure of the protein (Meyers, 2004). The amide I (C=O) band of bacterial proteins (Dowling et al., 1987) was detected in the biofilm formed by the pure SRB culture in Postgate C medium at 1,638 cm^{-1} as well as the amino acid side chains at 1,510 cm^{-1} (Al-Saadi et al., 2021b) (however, this could also be due to the structurally adsorbed water, as discussed earlier). The PO_4^{2-} symmetric stretching vibration of phosphates was detected in the region (~1,085 cm^{-1}). Vibrations due to the carbohydrate backbone also occurred in the region between 1,184 cm^{-1} to 1,002 cm^{-1}. The "fingerprint region" refers to the spectral range 900 to 600 cm^{-1} and contains weakly expressed bands arising from the aromatic ring vibrations of nucleotides (Naumann and John WileySons, 2006) and the CH_2 rocking vibration of lipids (Coates, 2000; Socrates, 2000; Meyers, 2004; Naumann and John WileySons, 2006).

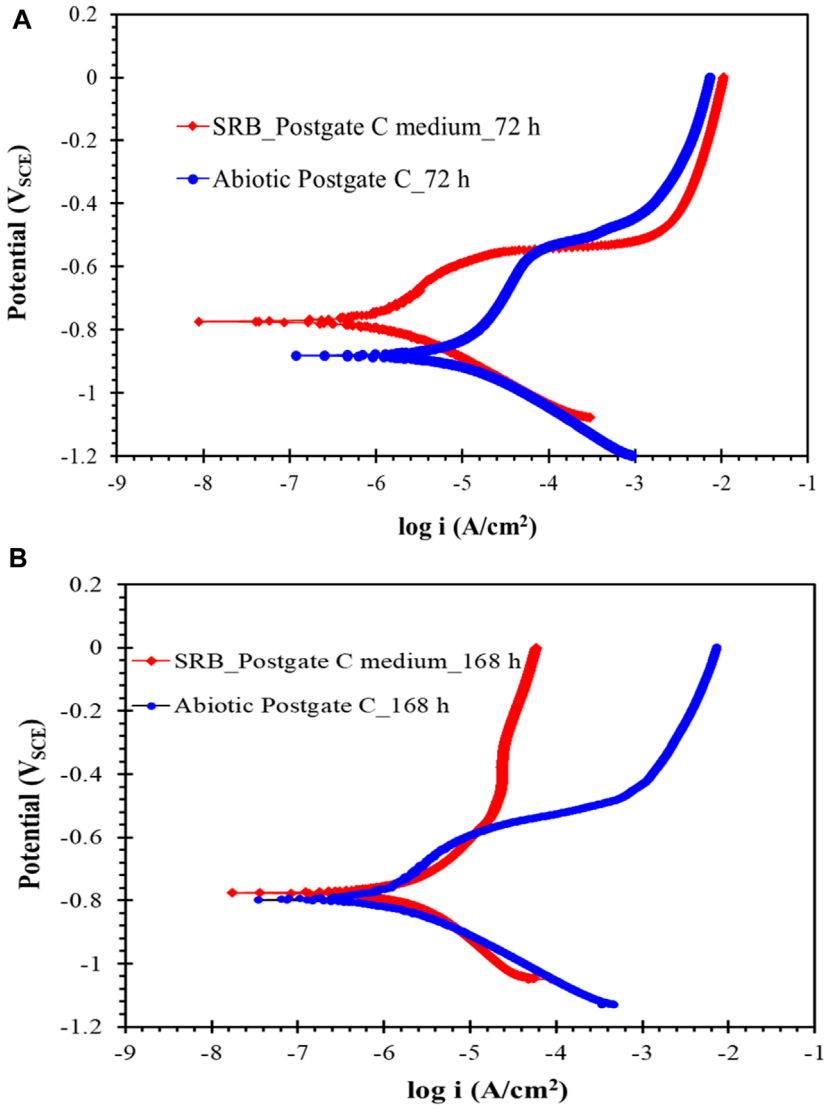

FIGURE 7
Potentiodynamic polarization scan of carbon steel after **(A)** 72 h and **(B)** 168 h of exposure to common Postgate C medium with and without the SRB culture.

Cross sectional analysis using FIB-SEM (Figure 4) shows the corroded surface under the SRB biofilm. Pitting appeared to be initiated under the SRB biofilm at the areas shown in Figures 4B,C. Both pit mouths in the cross section appeared to have two layers of biofilm; one layer covered the pit mouth while the other covered the whole. At the 72 h stage, pits had not yet progressed to become deep or well defined. The biofilm contained cracks and some porosity was observed adjacent to areas of compact film. Pores observed in Figures 4B,C would better allow aggressive ions such as S^{-2} and Cl^{-} in the electrolyte to come in contact with the bare metal, and hence, would be expected to enhance pitting corrosion. EDS analysis in Figure S2 shows the presence of oxygen and sulphur, suggesting that iron oxyhydroxides and iron sulphide were present in the material covering the pit following 72 h immersion.

The term tubercle is defined as a small-rounded prominence and has been used previously to describe corrosion product deposits (Ray et al., 2010). The tubercle formed in the SRB biofilm Figure 4D had a build-up of biological material within the core intertwined with corrosion products. It is widely reported in literature that the area under a tubercle is deprived of oxygen and acts as an anode to the surrounding cathodic area, which leads to pitting corrosion of carbon steel (Little et al., 2010; Ray et al., 2010). Localised pitting corrosion, however, had not occurred under the deposit in Figure 4D due to the initial iron oxide layer remaining intact. Therefore, FIB-SEM technique has clearly shown that the presence of tubercles on carbon steel does not always lead to pitting corrosion underneath. The fundamental mechanisms of SRB-influenced deterioration of steel have been based on the activity of hydrogenase enzymes and/or the existence of iron sulphide

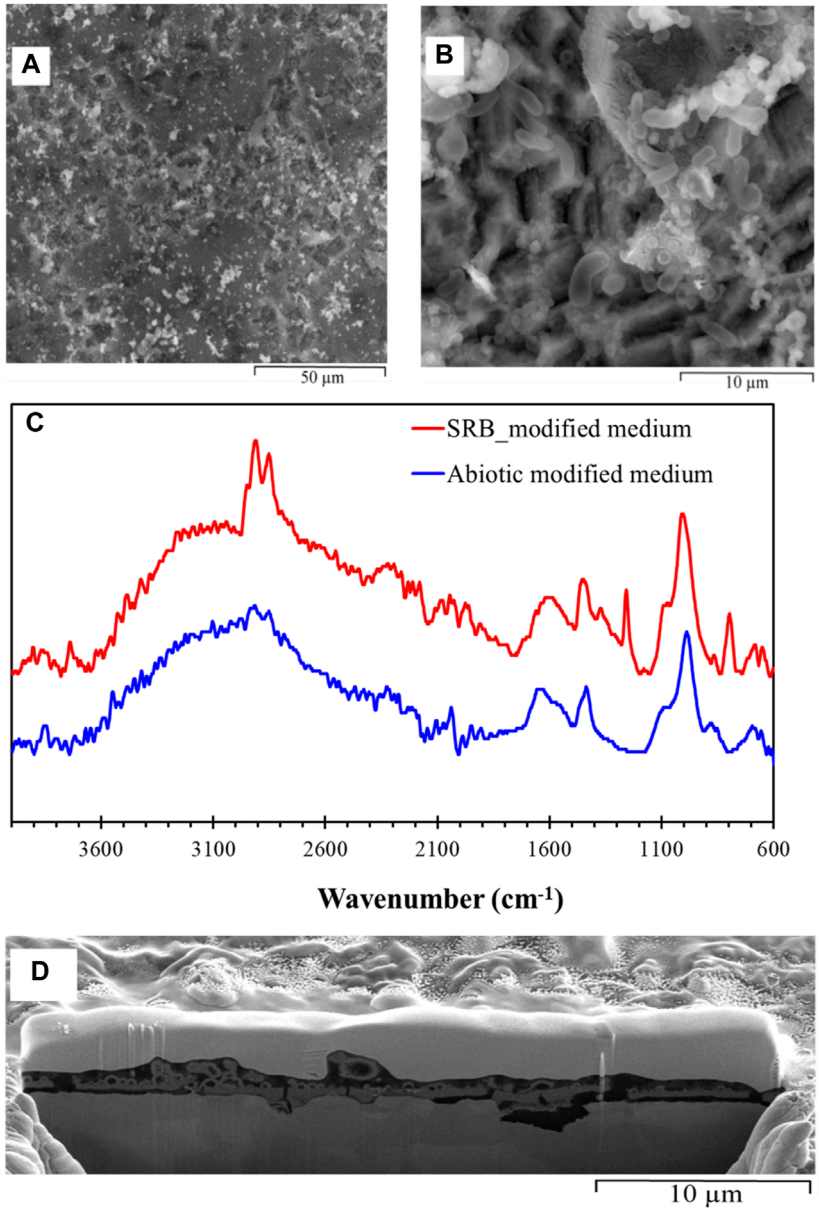

FIGURE 8
ESEM images of hydrated biofilm formed on carbon steel by a pure SRB culture following 72 h exposure in modified Postgate C medium: **(A)** porosities in the SRB biofilm and **(B)** SRB cells scatted across the specimen, **(C)** IR spectra of SRB biofilm formed on carbon steel exposed to pure SRB culture in modified Postgate C medium for a period of 72 h, and **(D)** FIB-SEM, Cross-sectional analysis of biofilm formed on carbon steel by pure culture of SRB in modified Postgate C medium following a 72 h exposure.

species (Beech, 2003). The capacity of SRB to produce and utilize H_2 suggests that these microorganisms possess hydrogenase enzyme, which catalyses the reversible reaction in Eq. (2) (Pankhania, 1988; Beech, 2003).

$$2H^+ + 2e^- = 2[H] = H_2 \quad (2)$$

The detection of hydrogenase in the biofilms can be attributed to the shift from chemo-organic to chemo-lithotrophic metabolism by some organisms present in the mixed biofilm inhabitants as a result of the low levels of consumed carbon sources; lactate or acetate remained in the recycling medium. The induction of hydrogenase activity was probably due to the ability of those organisms to use cathodically produced hydrogen as an alternative energy source (Bryant et al., 1991). The most relevant effects of SRB metabolites on corrosion (Videla, 2000) would include providing several sulphur compounds that constitute corrosive anions for steel and iron, and producing aggressive final metabolic products (sulfides, bisulfides, hydrogen sulfides) or intermediate metabolites such as thiosulfate and polythionates. Moreover, through biological and inorganic transformation paths, SRB metabolites change to sulfide anions that are corrosive to iron and steel. The characteristics and intensity of sulfide action are closely connected to the nature of the pre-existing passive film on the metal surface (Videla et al., 2004). Other ions (e.g., chlorides) in the medium enhance the

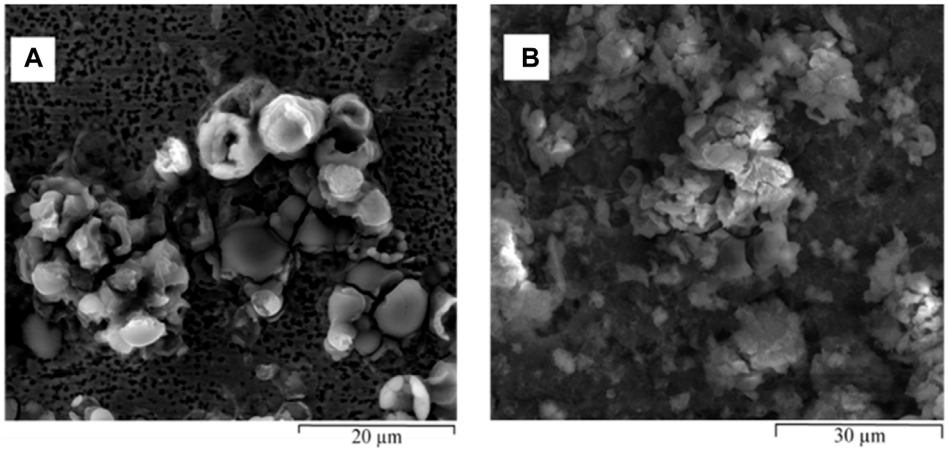

FIGURE 9
ESEM images of different locations of hydrated biofilm formed on carbon steel by a pure SRB culture following 168 h exposure in modified Postgate C medium: **(A)** extensive pitting attack on the carbon steel and **(B)** SRB biofilm rich in iron sulphides.

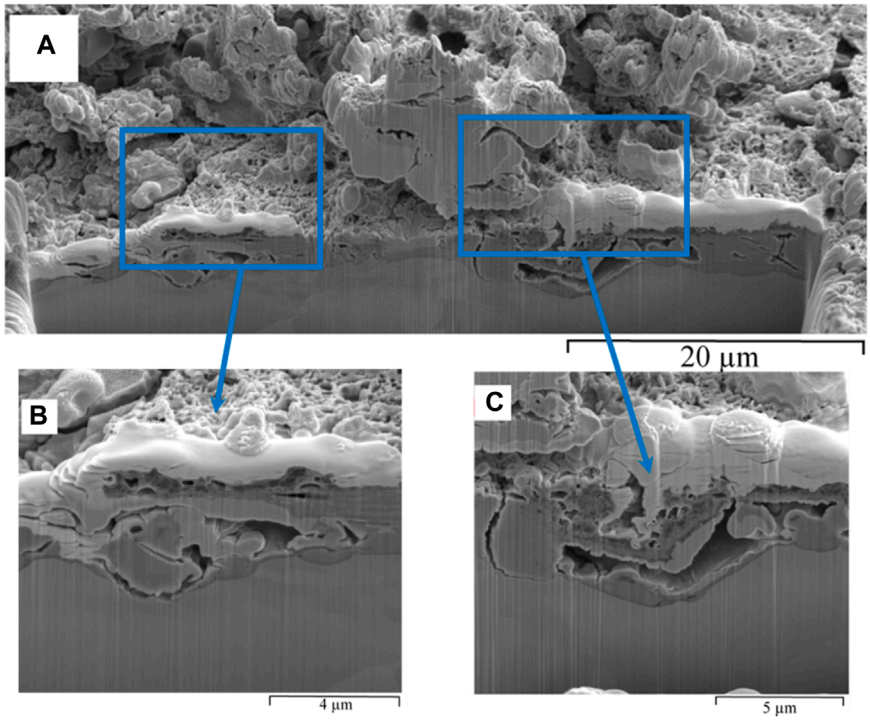

FIGURE 10
FIB-SEM, cross-section of biofilm formed on carbon steel by pure culture of SRB in modified Postgate C medium following a 168 h exposure: **(A)** overview of the cross section, and **(B)** and **(C)** close view of hollow voids in the biofilm.

participation of sulfide in the corrosion process (Videla and Characklis, 1992).

Figures 5A,B depict the ESEM micrograph of carbon steel exposed to SRB for 168 h. Extensive pitting (with a shallow pit morphology, as seen in Figure 5C) was observed. The biofilm varied in thickness with areas of high thickness containing porous deposits observed alongside tightly adherent film. The detection of sulphur in the SRB biofilm, by EDS analysis (Figure S3), suggested that over time, sulphide ions were incorporated into SRB biofilms which were initially rich in iron oxides and/or iron hydroxides. The highly nutritious conditions in the bulk media meant that the bacteria within the biofilm did not pre-require attachement to the metal surface. EDS also detected other elements present in the bacterial cell body (viz; C, O, S, and P) (Li et al., 2020). The cross-section of

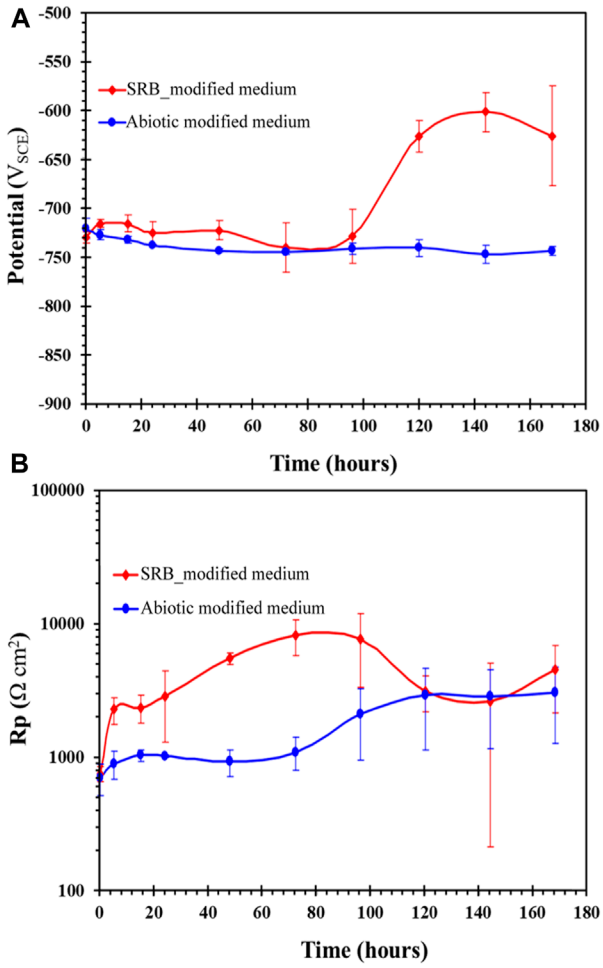

FIGURE 11
Carbon steel exposed to modified Postgate C medium with and without SRB culture, showing with time change in: **(A)** OCP and **(B)** linear polarisation resistance.

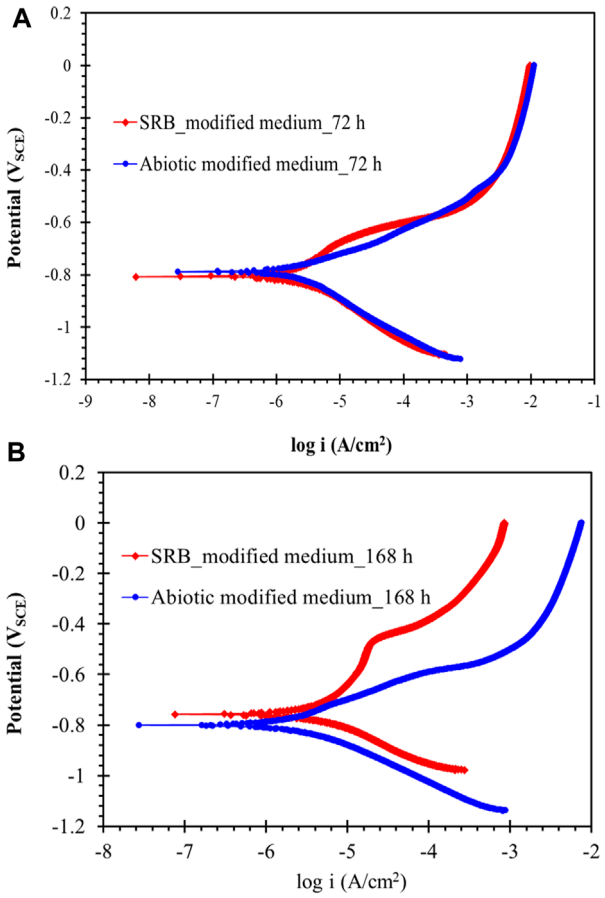

FIGURE 12
Potentiodynamic polarisation scan of carbon steel after **(A)** 72 h and **(B)** 168 h of exposure to a pure SRB culture in modified Postgate C medium.

the 168 h SRB biofilm in Postgate C medium (Figure 5C) showed the porosity in film was greater as compared to the film observed at 72 h.

3.2.2 Electrochemical characterization of carbon steel in Postgate C medium

Electrochemical information on the evolving biofilm formation was monitored non-destructively using the linear polarisation technique. The polarisation resistance (R_p) monitored over a 72 h period is shown in Figure 6. The standard deviation of the R_p data for the SRB biofilm was significantly greater than that for the abiotic film. Subsequent to the 72-h reading, R_p oscillated considerably and reproducible data could not be obtained. R_p data obtained from linear polarisation technique should only be converted into corrosion rate if uniform corrosion occurs, the solution is highly conductive and no scale/deposits are present on the surface (Hilbert et al., 2007). As can be observed from earlier ESEM analysis (Section 3.2.1), the formation of a heterogeneous biofilm, developed over 72 h exposure and thereafter, meant that the LPR technique could only be used qualitatively for this study. Hence, the increase in R_p can be taken as a sign of an apparent passive film forming on the surface of the carbon steel which offered mass transfer resistance to active anodic dissolution. Newman et al. (Newman et al., 1992) observed that in high sulphide environments, low alloy carbon steel passivated to give in R_p values over 50,000 Ω/cm^2.

The potentiodynmic polarisation curve for carbon steel following 72 h exposure to SRB environment is shown in Figure 7A. The corrosion potential (E_{corr}) shifted to more positive potentials for the carbon steel coupon exposed to common Postgate C solution with SRB compared to steel immersed in abiotic solution. The corrosion current density (I_{corr}) of carbon steel in abiotic solution was more than 6x higher than that of steel in biotic solution. The improvement in corrosion resistance of carbon steel in biotic solution is attributed to the development of protective FeS film on carbon steel surface, which is consistent with the reported literature (Al-Saadi et al., 2017; Al-Saadi and Raman, 2019). However, consequent to application of an anodic scan the film was disrupted at around −0.6 V_{SCE} and active corrosion followed thereafter.

In contrast, the anodic curve of the potentiodynamic polarisation scan following 168 h exposure (Figure 7B) showed resistance to the anodic dissolution when the corrosion potential was increased positive of −550 mV. Due to the adherent film of iron sulphides which acted as a diffusive barrier to reactants, the

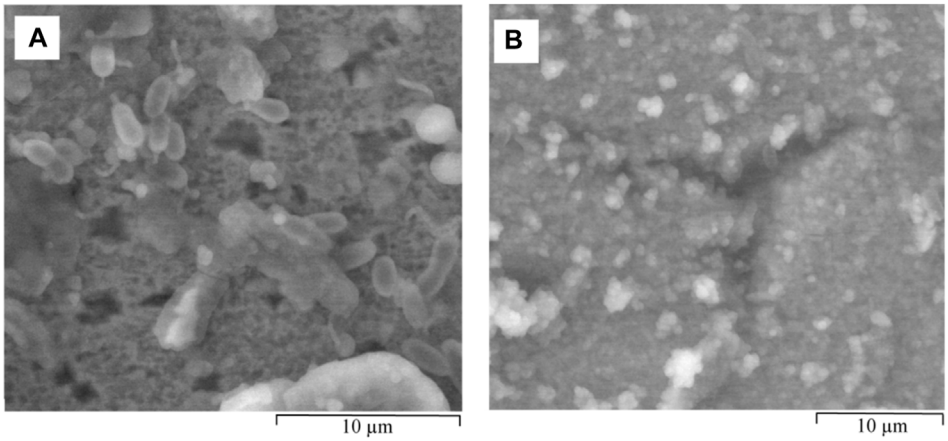

FIGURE 13
ESEM images of hydrated biofilm formed on carbon steel by a pure SRB culture following 72 h exposure in inorganic medium. **(A)** dwarf bacterial cells scattered alongside shallow pits and **(B)** areas susceptible to localised corrosion due to breaks in the SRB biofilm.

anodic current was lower at higher overpotentials under the SRB environment as compared to the abiotic condition. The mechanism of development of the robust iron sulphide film upon application of anodic overpotential is well-covered in the literature (Al-Saadi et al., 2017; Al-Saadi and Raman, 2019; Al-Saadi et al., 2021a).

3.3 Biofilm and electrochemical characterization in modified Postgate C medium

3.3.1 Biofilm characterization in modified Postgate C medium

When cultured in modified Postgate C medium (Postgate C, without the organic nutrient yeast extract), the biofilms with much greater porosity content were observed (Figure 8) and a significantly greater number of bacterial cells were observed on the metal surface following 72 h exposure as seen in Figure 8B. Pitting and surface roughness are apparent throughout the biofilm. EDS (Figure S4) was taken on a colony of bacteria showing a high carbon content, confirming the presence of biological cells and EPS present in the biofilm.

In contrast to the SRB biofilm developed in Postgate C medium, the relatively slower growth of the SRB in the modified Postgate C medium resulted in thinner film and hence weak signals for biomolecules in the IR spectra (Figure 8C). Typical thickness of this SRB biofilm was ≈500 nm as seen in Figure 8D. Ideal thickness for the ATR-FTIR is ≥1 μm. However, ATR-FTIR analysis in Figure 8C was able to discern weak signals enabling some information regarding the IR active functionality of the biofilm to be investigated. The IR signal obtained for the SRB biofilm in modified Postgate C medium showed the presence of hydrocarbons, carbohydrates, phosphates and amide groups due to proteins.

Cross-sectional images show the presence of initial porous layer of corrosion product layer which was primarily iron oxyhydroxides (Figure 8D). Videla has reported that 48–72 h biofilms formed in laboratory conditions generally contain spherules of colloidal goethite and crystalline hematite (Videla, 2001). Magnetite (Fe_3O_4) and ferrous hydroxide ($Fe(OH)_2$) have also been observed in previous studies (Lee et al., 1993). Iron oxyhydroxides is reported to be protective in stable films on iron (Foroulis, 1980; Jones, 1996; Revie, 2008; Sato and Sharma, 2012). FIB-SEM analysis in Figure 8D clearly shows that pitting corrosion occurred at locations of breakage in the iron oxyhydroxide film which allowed the chemical species to reach the carbon steel and cause corrosion. The breakdown of passive films is a complex problem and currently there is no single accepted mechanism. The passive iron oxide film may have broken down due to penetration (Strehblow and Marcus, 2002) or adsorption (Szklarska-Smialowska, 1986; Strehblow and Marcus, 2002) of aggressive anions from the media (such as sulphide and chloride) into the film or as a result of direct access of these ions to the metal substrate due to disruptions in the passive film (Strehblow and Marcus, 2002; Sato and Sharma, 2012). Previous studies have reported mackinawite (FeS_{1-x}) to be the first iron sulphide to form (King and Miller, 1977; Yuan et al., 2013) and considered responsible for breakdown in passivity when exposed to SRB (Videla, 1987).

Figure 9 shows the ESEM micrographs of carbon steel exposed for 168 h to the modified biotic Postgate C solution (Postgate C without yeast). The ESEM image in Figure 9A shows extensive pitting following 168 h exposure. Surface coverage was greater in this case (Figure 9B) than for the 72 h biofilm (Figure 8B). EDS results in Figure S5 shows high sulphur and iron contents, suggesting iron sulphide incorporation into the SRB biofilm. Rapid H_2S formation occurred when SRB was cultured in nutrient rich Postgate C medium; however, EDS analysis consistently showed a higher ratio of sulphur incorporated into the 168 h SRB biofilm in the modified Postgate C medium which contained fewer organic nutrients. This may be due to attached bacterial cells as observed in the biofilm formed in nutrient-deficient Postgate C medium, but not observed when cultured in the Postgate C medium. The attached bacterial cells were probably able to concentrate H_2S into the biofilm more effectively than planktonic cells. It is widely reported that once the iron sulphide species make contact with carbon steel, galvanic corrosion occurs where the iron sulphide

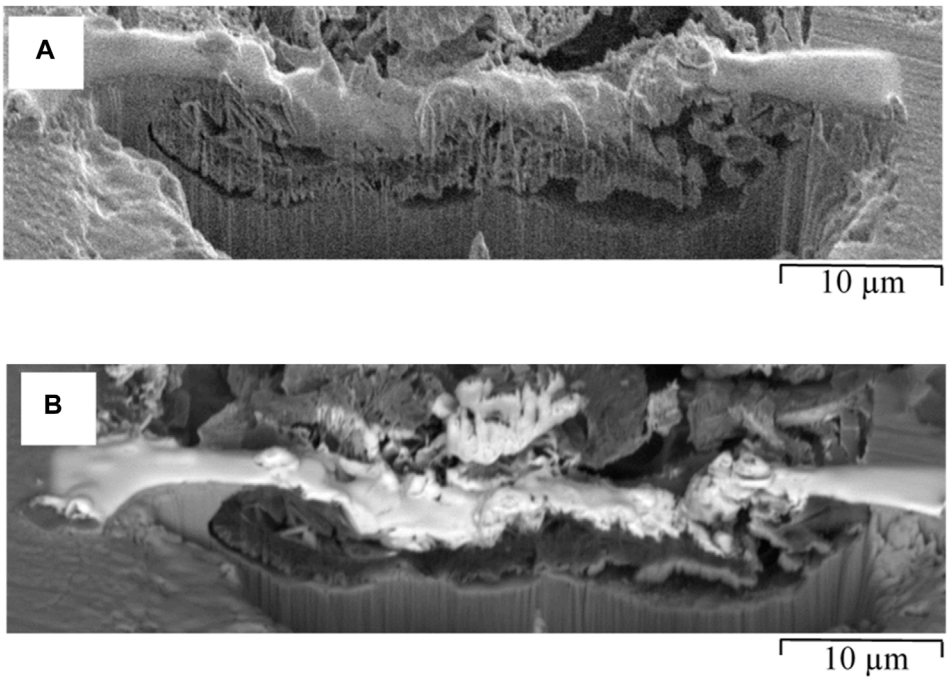

FIGURE 14
FIB-SEM, cross-section of biofilm formed on carbon steel by pure culture of SRB in inorganic medium following a 72 h exposure: **(A)** secondary electron image and **(B)** back scatter image.

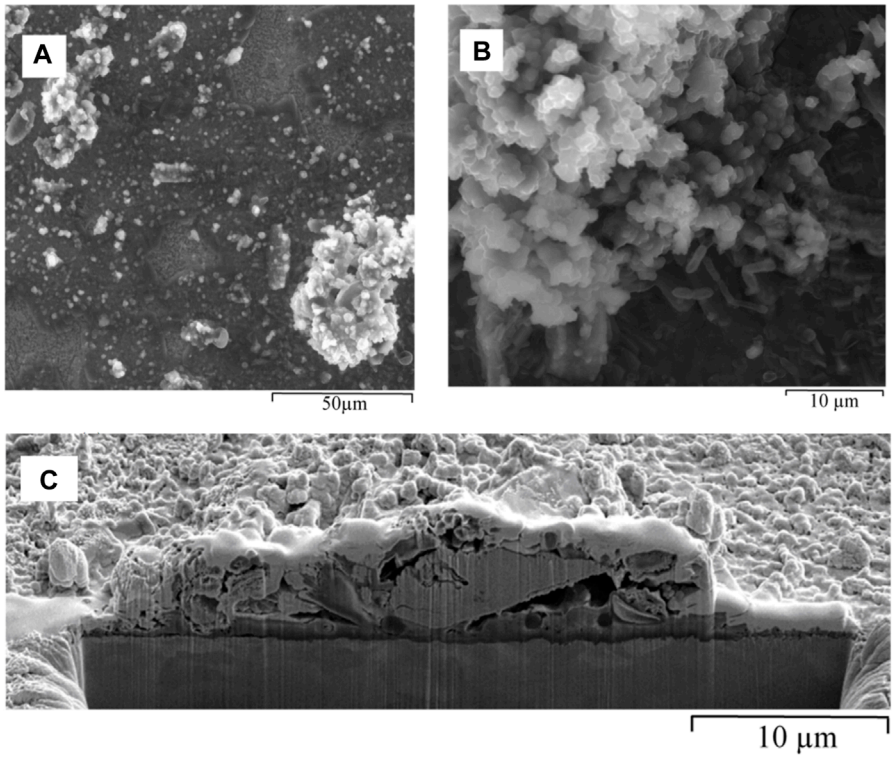

FIGURE 15
ESEM images of hydrated biofilm formed on carbon steel following 168 h exposure in inorganic medium with a pure SRB culture: **(A)** an overview of the biofilm showing breaks in the film and inorganic/organic precipitates and **(B)** colonies of dwarf bacterial cells under a biofilm deposit. **(C)** FIB-SEM image of the cross-section of biofilm formed on carbon steel by pure culture of SRB in inorganic medium following a 168-h exposure.

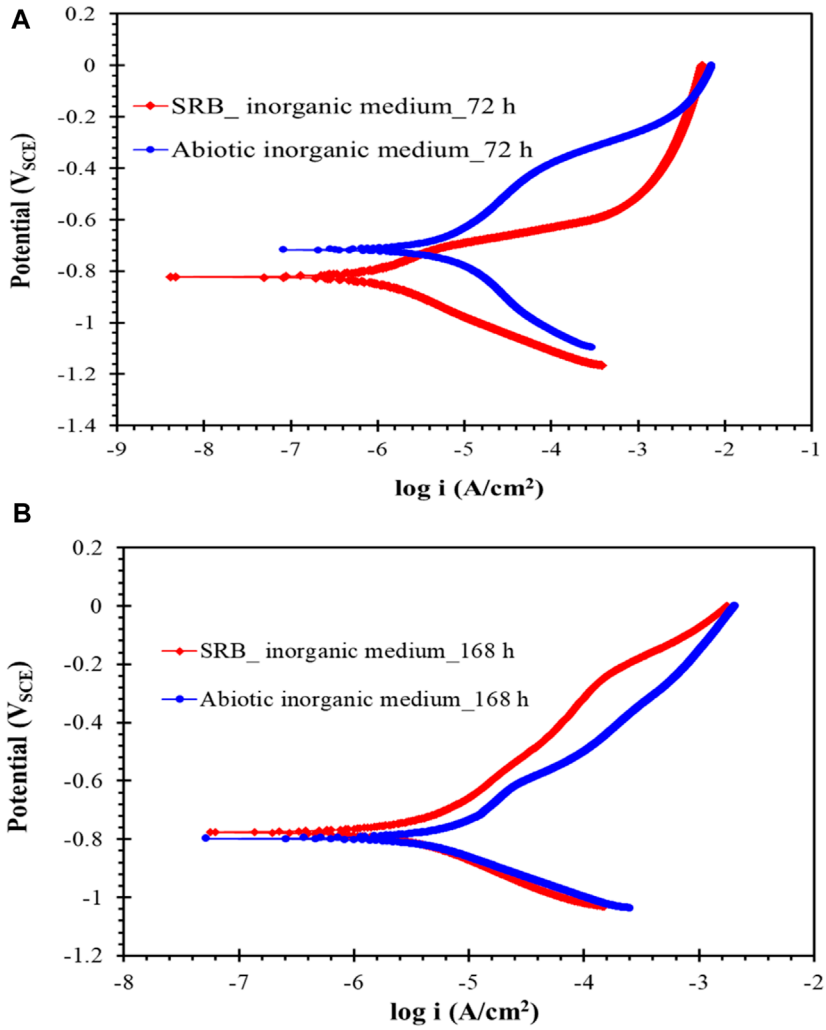

FIGURE 16
(A) and **(B)** Potentiodynamic polarisation scan of carbon steel after exposure to inorganic Postgate C solution without and with SRB culture for 72 and 168 h.

behaves as the cathode while the steel becomes the anode (Lee et al., 1993; Hilbert et al., 2007). Factors causing this galvanic corrosion include nobler potentials of iron sulphides, their semi-conducting properties, low overpotential for hydrogen reduction and common defects in the iron sulphide crystal structure (Hilbert et al., 2007). Heterogeneous thickness of the biofilm can be observed in Figure 10 as well. Some areas of the film (not shown) were as thick as 10 µm and were rich in elemental sulphur. Substructure features of this biofilm include hollow spaces and shrinkage-cracking which would allow contact with ions in solution.

3.3.2 Electrochemical characterization of carbon steel in modified Postgate C medium

Change in OCP with time is shown in Figure 12A. From 0 h to 96 h, the E_{corr} was relatively stable (~-726 mV). SRB growth was likely to be at exponential phase at around 72 h, as indicated by earlier results presented in Figure 1. However, E_{corr} was observed to increase suddenly after 96 h exposure exclusively to SRB containing medium, caused by iron sulphide precipitation. At 92 h, strong H_2S odour and heavy blackening of the solution was observed. The next E_{corr} reading at 120 h, after the blackening observed at 96 h, resulted in a significant increase in E_{corr} to −628 mV. This positive shift in E_{corr} of about 100 mV from the reading at 0 h may be due to the precipitation of iron sulphide on the carbon steel (Hack, 1988). Oscillations of E_{corr} were observed more commonly when taking OCP readings for SRB biofilm as compared to the abiotic control. This was an indication of localised corrosion in the presence of SRB, due to local rupture of the biofilm and/or transpassive dissolution (Fonseca et al., 1998).

The linear polarisation resistance measurement over the 168 h period is shown in Figure 11B. While the E_{corr} remained stable up to 96 h (Figure 11A), the corresponding R_p increased from 702 Ω.cm^2 at 0 h to 2,279 Ω.cm^2 at 5 h due to rapid precipitation of an initial iron sulphide film in the presence of the SRB. From 5 h to 96 h the R_p increased further as sulphides became increasingly incorporated into the biofilm. However, from 120 h to 168 h, where an increase in E_{corr} was observed through OCP measurement, the R_p decreased showing that the film was increasingly facilitating

corrosion over time as more H_2S was accumulated in the batch culture.

The potentiodynamic polarisation scan for the carbon steel following 72 h exposure to SRB in modified Postgate C medium (without yeast) showed active anodic and cathodic behaviour (Figure 12A) due to the lack of a protective passive SRB biofilm. There was no significant difference between the anodic and cathodic regime of the carbon steel exposed to abiotic control or the SRB containing medium. This result was consistent with the OCP results at 72 h (Figure 11A) where E_{corr} readings were also similar for both conditions. Although R_p was higher at 72 h in the SRB environment (Figure 11B), such resistance to anodic dissolution was not observed in the potentiodynamic polarisation results, since iron sulphide precipitates were insufficient in concentration to form a FeS layer on carbon steel upon application of anodic potential scan. However, over time, the concentration of H_2S and concurrent iron sulphide formation could be observed to increase, as confirmed by the blackening of the test solution (Figure 1) and H_2S odour. As in the case with the biofilms formed in Postgate C medium, the biofilm formed in modified Postgate C resisted uniform anodic dissolution during following 168 h (Figure 12B). The decrease in anodic rate occurred due to the precipitation of iron sulphide layer at high overpotentials which imposed mass transfer limitations to further anodic dissolution of the carbon steel. Pitting potential (E_p) could be observed at −450 mV. Unlike the biofilms formed under nutritionally rich Postgate C medium, the cathodic corrosion current density was higher than the abiotic control. Bacteria may influence the cathodic reactions by consumption or production of cathodic reactants such as oxygen and hydrogen (Videla, 2001). Tang et al. linked the increased H_2S formation by the SRB to promotion of the cathodic hydrogen evolution reaction on carbon steel (Tang et al., 2010). Increased bacterial cell attachment in the modified Postgate C medium as compared to the Postgate C medium may have had a role in concentrating the H_2S close to the metal surface and thus accelerating cathodic processes.

The modified Postgate C medium contained sufficient nutrients for the growth of SRB. However, limiting the organic nutrient content available for the bacteria by removing yeast extract slowed growth and hence, slowed the iron sulphide precipitation on carbon steel. The lower organic nutrient in the media aided attraction of bacterial cells to the carbon steel surface and hence significantly increased attachment to the alloy steel surface.

3.4 Biofilm and electrochemical characterization of carbon steel exposed to SRB medium without organic nutrients (inorganic medium)

Highly nutritional conditions such as those provided by commonly used laboratory media are rarely found in industrial systems (Padilla-Viveros et al., 2006). Therefore, the behaviour of SRB under oligotrophic (low organic nutrient) conditions was investigated by removing organic nutrients from the Postgate C media. In the absence of organic nutrients, H_2 and the residual nutrients coming from the inoculation present in the enrichment culture were the only possible electron donors available for the anaerobic SRB. Nielsen and Hilbert (Nielsen and Hilbert, 1997) have suggested that the hydrogenase enzyme in SRB, which facilitates the reduction of H_2, is only active under carbon nutrient limited conditions.

3.4.1 Biofilm characterization

SRB cells can be seen on the surface of the specimen in Figure 13A. However, due to insufficient nutrients in the inorganic medium, the bacterial cells were smaller in size (dwarf cells). In this state, the bacteria are not killed, but remain dormant until conditions become favourable (Oliver, 1993). A higher number of pits were found in the carbon steel exposed to SRB in the inorganic medium than in the other two culture media at 72 h. However, these pits were shallower than the pits formed under more nutrient sufficient conditions. Cracks in the biofilm which can likely lead to pitting corrosion were also observed (Figure 13B). EDS elemental analysis of this biofilm in Figure S6, corresponding to the area scattered with bacterial cells, detected high concentration of oxygen as well as phosphorous and inorganic magnesium.

The cross-section of a representative area of the biofilm (Figure 14A) shows a rough, corroded steel surface. The backscatter image in Figure 14B of the area seen in Figure 14A shows that the first corrosion product layer has a similar contrast to that of the bare metal. EDS analysis in Figure S7 showed that this film contains high levels of oxygen, sulphur and iron probably as a combination of iron sulphide and iron oxyhydroxide corrosion products. Shoesmith et al. showed that the H_2S absorbs at active oxide sites and may displace OH from the iron oxyhydroxide due to the sulphide ion's greater polarisability (Sherar, 2011).

Figures 15A,B depict ESEM images of hydrated biofilm developed on carbon steel exposed for 168 h to inorganic Postgate C solution with pure SRB. High concentration of inorganic precipitates as well as biological material was found on the surface of the coupon. Bacterial cells also attached to the surface as a coping strategy for unfavourable conditions. The shallow pits observed at 72 h exposure in the inorganic medium had become covered by corrosion deposits and therefore could no longer be seen. Cross-sectional analysis of the 168 h SRB biofilm (Figure 15C) did not show well-defined deep pitting as observed under more nutritionally favourable conditions. The lower ability of the SRB biofilm to attack carbon steel may be due to the weakened enzymatic activity of the starved SRB cells (Xu et al., 2023) under the condition.

3.4.2 Electrochemical behaviour carbon steel inorganic medium with SRB

Figures 16A,B show the potentiodynamic polarization plots of carbon steel exposed for 72 and 168 h to inorganic Postgate C solution with and without SRB. It can be seen that upon 72 h of exposure, there was very little resistance to anodic dissolution and, actually, corrosion rate was accelerated compared with the abiotic control. The low sulphide level at 72 h also appeared to have accelerated anodic process in the presence of SRB than that observed under abiotic conditions (Figure 16A). In 168 h, the relatively low accumulation of sulphide produced by the SRB as well as biofilm containing bacterial cells and EPS material offered some resistance to uniform corrosion as seen by the slightly lower anodic current (Figure 16B).

4 Conclusion

When developing microbial biofilms in a laboratory setting, the composition of the culture medium was found to be crucial in determining the characteristics of the resulting biofilm. Highly favourable nutrient conditions present in the Postgate C medium led to rapid, extensive growth of sulphate reducing bacteria (SRB) and, concurrently, a rapid iron sulphide production in solution. However, high nutrient conditions prevented bacterial cell attachment directly onto the steel surface. Electrochemical results in this case showed that biofilms formed on mild steel when exposed to the Postgate C for 72 h and 168 h or the nutrient-deficient Postgate C for 168 h offered resistance to anodic polarisation. However, through ESEM and FIB-SEM cross-sectional analysis, localised pitting attack could be observed under the biofilm due to disruptions of the passive film.

Iron sulphide was observed to play a vital role in SRB-induced corrosion. FIB-SEM analysis suggested that iron oxide was the initial corrosion product layer to form on the metal surface. FIB-SEM also suggested that the sites at which the bare metal made contact with the iron sulphide led to pitting corrosion. SRB cells were shown to be capable of indirectly influencing the corrosion of carbon steel even when grown under extremely unfavourable conditions, deficient in all organic nutrients. In this case, a low sulphide environment led to shallow pitting in 168 h. However, active corrosion and lack of a passive film could be observed electrochemically when SRB was cultured in an inorganic medium. Electrochemical results suggest that in the presence of pure SRB, limited pit development occurred under layers of iron oxyhydroxides and iron sulfide species where mass transfer limitations led to low anodic current over an extended range of potentials in polarisation curves.

Data availability statement

The original contributions presented in the study are included in the article/Supplementary Material, further inquiries can be directed to the corresponding author.

Author contributions

SW: Conceptualization, Data curation, Formal Analysis, Investigation, Methodology, Validation, Visualization, Writing–original draft. SA-S: Data curation, Formal Analysis, Investigation, Methodology, Software, Writing–original draft, Writing–review and editing. WG: Conceptualization, Formal Analysis, Investigation, Methodology, Supervision, Validation, Visualization, Writing–review and editing. CP: Investigation, Methodology, Supervision, Validation, Visualization, Writing–review and editing. RS: Funding acquisition, Project administration, Resources, Supervision, Writing–review and editing.

Funding

The author(s) declare that no financial support was received for the research, authorship, and/or publication of this article.

Conflict of interest

The authors declare that the research was conducted in the absence of any commercial or financial relationships that could be construed as a potential conflict of interest.

Publisher's note

All claims expressed in this article are solely those of the authors and do not necessarily represent those of their affiliated organizations, or those of the publisher, the editors and the reviewers. Any product that may be evaluated in this article, or claim that may be made by its manufacturer, is not guaranteed or endorsed by the publisher.

Supplementary material

The Supplementary Material for this article can be found online at: https://www.frontiersin.org/articles/10.3389/fmats.2024.1360869/full#supplementary-material

References

Allsopp, D., Seal, K. J., and Gaylarde, C. C. *Introduction to biodeterioration*. Cambridge, Cambridge University Press2004.

Al-Saadi, S., Banerjee, P. C., and Raman, R. S. (2017). Corrosion of bare and silane-coated mild steel in chloride medium with and without sulphate reducing bacteria. *Prog. Org. Coatings* 111, 231–239. doi:10.1016/j.porgcoat.2017.06.006

Al-Saadi, S., Raman, R. K. S., Anisur, M. R., Ahmed, S., Crosswell, J., Alnuwaiser, M., et al. (2021b). Graphene coating on a nickel-copper alloy (Monel 400) for microbial corrosion resistance: electrochemical and surface characterizations. *Corros. Sci.* 182, 109299. doi:10.1016/j.corsci.2021.109299

Al-Saadi, S., and Raman, R. S. (2019). A long aliphatic chain functional silane for corrosion and microbial corrosion resistance of steel. *Prog. Org. Coatings* 127, 27–36. doi:10.1016/j.porgcoat.2018.10.024

Al-Saadi, S., Raman, R. S., and Panter, C. (2021a). *A two-step silane coating incorporated with quaternary ammonium silane for mitigation of microbial corrosion of mild steel*. USA, ACS Omega.

Al-Saadi, S. H. M. (2013). *Silane coatings for mitigation of microbiologically influenced corrosion of mild steel*. Germany, Monash University.

American Public Health, A., Eaton, A. D., American Water Works, A., and Water Environment, F. (2005). *Standard methods for the examination of water and wastewater*. Washington, D.C.: APHA-AWWA-WEF.

Beech, I. B. (2003). Sulfate-reducing bacteria in biofilms on metallic materials and corrosion. *Microbiol. today* 30 (8), 115–117.

Blankemeier, A. R. (2011). *Characterization of Pseudomonas fluorescens biofilm*. Washington, The Ohio State University.

Bryant, R. D., Jansen, W., Boivin, J., Laishley, E. J., and Costerton, J. W. (1991). Effect of hydrogenase and mixed sulfate-reducing bacterial populations on the corrosion of steel. *Appl. Environ. Microbiol.* 57 (10), 2804–2809. doi:10.1128/aem.57.10.2804-2809.1991

Castaneda, H., and Benetton, X. D. (2008). SRB-biofilm influence in active corrosion sites formed at the steel-electrolyte interface when exposed to artificial seawater conditions. *Corros. Sci.* 50 (4), 1169–1183. doi:10.1016/j.corsci.2007.11.032

Cheng, Y., Rairdan, B., and Luo, J. (1998). Features of electrochemical noise generated during pitting of inhibited A516-70 carbon steel in chloride solutions. *J. Appl. Electrochem.* 28 (12), 1371–1375. doi:10.1023/a:1003456009378

Coates, J. (2000). *Interpretation of infrared spectra, a practical approach in Encyclopedia of analytical chemistry*. Chichester: John Wiley & Sons Ltd, 10815–10837.

Cui, L. Y., Liu, Z. Y., Xu, D. K., Hu, P., Shao, J. M., Du, C. W., et al. (2020). The study of microbiologically influenced corrosion of 2205 duplex stainless steel based on high-resolution characterization. *Corros. Sci.* 174, 108842. doi:10.1016/j.corsci.2020.108842

Dowling, N. J. E., Guezennec, J., and White, D. C. (1987). "Methods of insight into mechanisms of microbially influenced corrosion," in *Seventh international biodeterioration symposium* (Cambridge, UK: Elsevier Applied Science).

Enning, D., and Garrelfs, J. (2014). Corrosion of iron by sulfate-reducing bacteria: new views of an old problem. *Appl. Environ. Microbiol.* 80 (4), 1226–1236. doi:10.1128/aem.02848-13

Fonseca, I. T., Feio, M. J., Lino, A. R., Reis, M., and Rainha, V. L. (1998). The influence of the media on the corrosion of mild steel by Desulfovibrio desulfuricans bacteria: an electrochemical study. *Electrochimica Acta* 43 (1-2), 213–222. doi:10.1016/s0013-4686(97)00227-2

Foroulis, Z. (1980). Electrochemical behavior and corrosion of iron in aqueous sulfidic solution. *Mater. Corros.* 31 (6), 463–470. doi:10.1002/maco.19800310606

Hack, H. P. (1988). *Galvanic corrosion ASTM committee G-1 on corrosion of metals* USA, (ASTM Philadelphia).

Heidersbach, R. (2018). *Metallurgy and corrosion control in oil and gas production*. USA, John Wiley &.

Hilbert, L. R., Hemmingsen, T., Nielsen, L. V., and Richter, S. (2007). Reliability of electrochemical techniques for determining corrosion rates on carbon steel in sulfide media. *Corrosion* 63 (4), 346–358. doi:10.5006/1.3278388

Jain, D. K. (1995). Evaluation of the semisolid Postgate's B medium for enumerating sulfate-reducing bacteria. *J. Microbiol. methods* 22 (1), 27–38. doi:10.1016/0167-7012(94)00061-b

Javaherdashti, R. (2017), *Microbiologically influenced corrosion (MIC), Microbiologically influenced corrosion*. Germany, Springer, 29–79.

Johnston, S. L., and Voordouw, G. (2012). Sulfate-reducing bacteria lower sulfur-mediated pitting corrosion under conditions of oxygen ingress. *Environ. Sci. Technol.* 46 (16), 9183–9190. doi:10.1021/es3019594

Jones, D. A. (1996). *Principles and prevention of corrosion*. 2nd Edition. China, Prentice Hall.

King, R., and Miller, J. (1977). *Corrosion of ferrous metals by bacterially produced iron sulphides and its control by cathodic protection, Anti-Corrosion Methods and Materials*.

Lee, W., Lewandowski, Z., Morrison, M., Characklis, W. G., Avci, R., and Nielsen, P. H. (1993). Corrosion of mild steel underneath aerobic biofilms containing sulfate-reducing bacteria part II: at high dissolved oxygen concentration. *Biofouling* 7 (3), 217–239. doi:10.1080/08927019309386255

Li, Y., Feng, S., Liu, H., Tian, X., Xia, Y., Li, M., et al. (2020). Bacterial distribution in SRB biofilm affects MIC pitting of carbon steel studied using FIB-SEM. *Corros. Sci.* 167, 108512. doi:10.1016/j.corsci.2020.108512

Little, B., Lee, J., and Ray, R. (2007). A review of 'green'strategies to prevent or mitigate microbiologically influenced corrosion. *Biofouling* 23 (2), 87–97. doi:10.1080/08927010601151782

Little, B., Ray, R., and Lee, J. (2010). *Tubercles and localized corrosion on carbon steel*. China, NAVAL RESEARCH LAB STENNIS SPACE CENTER MS OCEANOGRAPHY DIV.

Little, B. J., Blackwood, D. J., Hinks, J., Lauro, F. M., Marsili, E., Okamoto, A., et al. (2020). Microbially influenced corrosion—any progress? *Corros. Sci.* 170, 108641. doi:10.1016/j.corsci.2020.108641

Little, B. J., and Lee, J. S. (2009). *Microbiologically influenced corrosion*. China, NAVAL RESEARCH LAB STENNIS SPACE CENTER MS OCEANOGRAPHY DIV.

Little, B. J., and Lee, J. S. (2014). Microbiologically influenced corrosion: an update. *Int. Mater. Rev.* 59 (7), 384–393. doi:10.1179/1743280414y.0000000035

Little, B. J., and Lee, J. S. (2007). *Microbiologically influenced corrosion*. USA, John Wiley &.

Meyers, R. A. (2004). "FTIR of biomolecules," in *Encyclopedia of molecular cell biology and molecular medicine* (Weinheim.: Wiley-VCH Verlag GmbH & Co.).

Naumann, D. (2006). "Infrared spectroscopy in microbiology," in *Encyclopedia of analytical Chemistry2006*. Editors L. John Wiley, Sons.

Newman, R., Rumash, K., and Webster, B. (1992). The effect of pre-corrosion on the corrosion rate of steel in neutral solutions containing sulphide: relevance to microbially influenced corrosion. *Corros. Sci.* 33 (12), 1877–1884. doi:10.1016/0010-938x(92)90190-e

Nielsen, L. V., and Hilbert, L. R. (1997), Microbial corrosion of carbon steel by sulfate-reducing bacteria:: electrochemical and mechanistic approach, Aspects of microbially induced corrosion, *Inst. Mater.*, 1997, 11–24.

Ojeda, J. J., Romero-González, M. E., and Banwart, S. A. (2009). Analysis of bacteria on steel surfaces using reflectance micro-fourier transform infrared spectroscopy. *Anal. Chem.* 81 (15), 6467–6473. doi:10.1021/ac900841c

Oliver, J. D., (1993), *Formation of viable but nonculturable cells, Starvation in bacteria*, Germany, Springer, pp. 239–272.

Padilla-Viveros, A., Garcia-Ochoa, E., and Alazard, D. (2006). Comparative electrochemical noise study of the corrosion process of carbon steel by the sulfate-reducing bacterium Desulfovibrio alaskensis under nutritionally rich and oligotrophic culture conditions. *Electrochimica Acta* 51 (18), 3841–3847. doi:10.1016/j.electacta.2005.11.001

Pankhania, I. P. (1988). Hydrogen metabolism in sulphate-reducing bacteria and its role in anaerobic corrosion. *Biofouling* 1 (1), 27–47. doi:10.1080/08927018809378094

Papavinasam, S. (2013), *Corrosion control in the oil and gas industry*. China, Elsevier.

Pinney, N., and Morgan, D. (2013). *Ab initio* study of structurally bound water at cation vacancy sites in Fe- and Al-oxyhydroxide materials. *Geochimica Cosmochimica Acta* 114, 94–111. doi:10.1016/j.gca.2013.03.032

Ramesh, A., Lee, D.-J., and Hong, S. G. (2006). Soluble microbial products (SMP) and soluble extracellular polymeric substances (EPS) from wastewater sludge. *Appl. Microbiol. Biotechnol.* 73 (1), 219–225. doi:10.1007/s00253-006-0446-y

Ray, R. I., Lee, J. S., Little, B. J., and Gerke, T. (2010). The anatomy of tubercles: a corrosion study in a fresh water estuary. *Mater. Corros.* 61 (12), 993–999. doi:10.1002/maco.201005739

Revie, R. W. (2008). *Corrosion and corrosion control: an introduction to corrosion science and engineering*. USA, John Wiley &.

Sato, N. (2012). "Green corrosion chemistry and engineering: opportunities and challenges," in *Wiley-VCH verlag GmbH & Co*. Editor S. K. Sharma USA, (KGaA), 3.

Sherar, B. (2011). *The effect of the environment on the corrosion products and corrosion rates on gas transmission pipelines*.

Socrates, G. (2000). *Infrared and Raman characteristic group frequencies: tables and charts*. Third Edition. New York: Chichester.

Steve, R., and Robert, P. (2001). A review of focused ion beam applications in microsystem technology. *J. Micromechanics Microengineering* 11 (4), 287–300. doi:10.1088/0960-1317/11/4/301

Strehblow, H.-H., and Marcus, P. (2002). Mechanisms of pitting corrosion. *Corros. TECHNOLOGY-NEW YORK BASEL-*, 17, 243–286.

Szklarska-Smialowska, Z. (1986). *Pitting corrosion of metals*, 69–96. Houston: NACE, 431.

Tang, J., Shao, Y., Guo, J., Zhang, T., Meng, G., and Wang, F. (2010). The effect of H2S concentration on the corrosion behavior of carbon steel at 90°C. *Corros. Sci.* 52 (6), 2050–2058. doi:10.1016/j.corsci.2010.02.004

van Houten, R. T. *Biological sulphate reduction with synthesis gas*. Wageningen, Wageningen University and Research1996.

Videla, H. (2018), *Manual of biocorrosion*. USA, Routledge.

Videla, H. A. (1987). "Electrochemical Interpretation of the role of microorganisms in corrosion," in *Seventh international biodeterioration symposium* (Cambridge, UK: Elsevier Applied Science).

Videla, H. A. (2000). An overview of mechanisms by which sulphate-reducing bacteria influence corrosion of steel in marine environments. *Biofouling* 15 (1-3), 37–47. doi:10.1080/08927010009386296

Videla, H. A. (2001). Microbially induced corrosion: an updated overview. *Int. Biodeterior. Biodegrad.* 48 (1-4), 176–201. doi:10.1016/s0964-8305(01)00081-6

Videla, H. A., and Characklis, W. G. (1992). Biofouling and microbially influenced corrosion. *Int. Biodeterior. Biodegrad.* 29 (3), 195–212. doi:10.1016/0964-8305(92)90044-o

Videla, H. A., and Herrera, L. K. (2004). "Chapter 7 biocorrosion," in *Studies in surface science and catalysis*. Editors R. Vazquez-Duhalt, and R. Quintero-Ramirez Germany, (Elsevier), 193–218.

Xu, D., and Gu, T. (2014). Carbon source starvation triggered more aggressive corrosion against carbon steel by the Desulfovibrio vulgaris biofilm. *Int. Biodeterior. Biodegrad.* 91, 74–81. doi:10.1016/j.ibiod.2014.03.014

Xu, D., Gu, T., and Lovley, D. R. (2023). Microbially mediated metal corrosion. *Nat. Rev. Microbiol.* 21, 705–718. doi:10.1038/s41579-023-00920-3

Yuan, S., Liang, B., Zhao, Y., and Pehkonen, S. (2013). Surface chemistry and corrosion behaviour of 304 stainless steel in simulated seawater containing inorganic sulphide and sulphate-reducing bacteria. *Corros. Sci.* 74, 353–366. doi:10.1016/j.corsci.2013.04.058